Insights into design of mobility control for chemical enhanced oil recovery

Farajzadeh, R.; Wassing, B. L.; Lake, L. W.

DOI
10.1016/j.egyr.2019.05.001

Publication date
2019

Document Version
Final published version

Published in
Energy Reports

Energy Reports 5 (2019) 570–578

Contents lists available at ScienceDirect

Energy Reports

journal homepage: www.elsevier.com/locate/egyr

Research paper

Insights into design of mobility control for chemical enhanced oil recovery

R. Farajzadeh [a,b,*], B.L. Wassing [b], L.W. Lake [c]

[a] Delft University of Technology, The Netherlands
[b] Petroleum Development Oman, Oman
[c] University of Texas at Austin, United States

ARTICLE INFO

Article history:
Received 27 February 2019
Received in revised form 26 April 2019
Accepted 6 May 2019
Available online xxxx

ABSTRACT

This study compares two methods of mobility-control design for chemical enhanced oil recovery processes. Method 1 matches the total relative fluid mobility upstream and downstream of the shock front. In method 2 the viscosity of the displacing agent is selected such that the total mobility at the shock water saturation is equal to or less than the minimum mobility across the saturation range. The two methods are based on fractional flow analysis of one-dimensional flow and they are validated against two-dimensional simulations of flow through heterogeneous permeable media. Our results emphasize the key role of the water/oil relative permeability curves for the design of mobility control in polymer and surfactant/polymer flooding. The polymer viscosity obtained by setting the shock-front mobility ratio to one (method 1) is the minimum viscosity to ensure a stable displacement front. Design by method 2 results in a larger viscosity than method 1. This shifts the shock water saturation to larger values and hence more oil is displaced. Moreover, we find that for surfactant-polymer (SP) solutions with ultra-low interfacial tension (IFT) reduction (Winsor type III), the required polymer viscosity is always greater than the oil viscosity (at low shear rates). However, for Winsor type I solutions, for oils with medium and large viscosity the non-linear shape of the relative permeability function leads to polymer viscosities that are less than that of the oil. For light oils the viscosity of the ASP solution should be significantly larger than the oil viscosity.

1. Introduction

Efficient extraction of oil from subsurface formations depends on (1) the displacement or microscopic sweep efficiency (determined largely by the mobility ratio between the displacing agent and the in-situ fluids and reductions in the interfacial tension) and (2) the macroscopic sweep efficiency, which for a homogeneous medium, depends on the stability of the displacement front (Bedrikovetsky, 1993; Lake et al., 2014). The mobility ratio is defined as the relative mobility (the quotient of the relative permeability and viscosity of the phase) of the injected or displacing fluid divided by that of the displaced fluid (Dake, 1978; Lake et al., 2014). For an immiscible displacement, when the capillary length is negligible compared to length of the system, an "abrupt" interface (or so-called shock front) separates two regions of large and small saturation of the displacing fluid. For any given time, the position of the shock front depends on its specific velocity, which equals the slope of the tangent line to the fractional-flow function originating from the initial saturation in the porous medium (see Fig. 1, left).

The overall balance of the forces acting on the interface, i.e., viscous, capillary, and gravity forces along with dispersion govern the stability of this front. In general, when the destabilizing forces (e.g. viscous forces) dominate the stabilizing forces (e.g. the capillary and dispersive forces), the microscopic perturbations caused by small-scale heterogeneities, can lead to development of fingers, and thus bypassing of the oil in place (Chouke, 1959; Homsy, 1987). When viscous forces dominate, the mobility ratio is used to evaluate the front stability. But the phase mobility depends on its saturation, so the saturation at which this ratio is evaluated could be very important.

The total (relative) mobility is defined as

$$\lambda_T(S_w) = \frac{k_{rw}(S_w)}{\mu_w} + \frac{k_{ro}(S_w)}{\mu_o} \quad (1)$$

In this equation, $k_{r\alpha}$ is the relative permeability and μ_α is the viscosity of phase α. Throughout this paper the displacing and displaced fluids are denoted by w and o, respectively. The solid line

* Correspondence to: Department of Geoscience & Engineering, Delft University of Technology, The Netherlands.
E-mail address: r.farajzadeh@tudelft.nl (R. Farajzadeh).

https://doi.org/10.1016/j.egyr.2019.05.001

in Fig. 1 (right) shows the total mobility (defined by Eq. (1)) corresponding to the saturation profile obtained from the Buckley–Leverett solution. Behind the shock front starting from point *A*, the total mobility increases continuously towards the injector (point *C*) for the case of $\lambda_o<\lambda_w$. The magnitude of the change depends on the relative permeability and the viscosity ratio of the phases. The general consensus is that for the shock front to remain stable, the total mobility upstream of the front should be less than that of downstream of the front, i.e.,

$$\lambda_T\left(S_w^A\right) \le \lambda_T\left(S_w^B\right) \text{ or } \frac{\lambda_T\left(S_w^A\right)}{\lambda_T\left(S_w^B\right)} \le 1 \tag{2}$$

In other words, the mobility ratio across the shock should be less than one. The stability condition in Eq. (2) applies strictly to the front. As long as the mobility ratio at point *C* (the injection point) is larger than unity, fingers will be initiated and propagate within the region behind the front. However, for immiscible displacement, the growth of these fingers might not be fast enough to affect the front stability (Farajzadeh et al., 2016).

Fig. 2 shows simulation results of water displacing oil, for a case where the mobility at point *A* is twice that of point *B*, i.e., for a shock mobility ratio of 2. As expected, once water is injected into the medium, fingers are initiated and then grow relative to the average speed of front (Riaz and Tchelepi, 2004, 2006) until they reach the producer at the right side. In Fig. 3 we choose the relative permeability parameters such that the total mobility's at points *A* and *B* match, i.e., the mobility ratio across the shock front becomes one. For this case, the front remains stable; however, because the end-point mobility ratio (the ratio between the relative mobility of the displacing fluid at the injection point and the relative mobility of the oil at irreducible water saturation) is still greater than 1 fingers are initiated within the bank behind the front, but they do not reach the front, most likely because their growth is relative to the speed of the saturations within the finger, which propagate slower than the shock-front saturation. In fact the so-called Buckley–Leverett tail (or rarefaction solution) is a form of instability behind the shock front; however, the growth of these instabilities are not fast enough to overtake the front (Riaz and Tchelepi, 2004).

Injection of water into reservoirs containing oils with small mobility (large viscosity) can suffer from instabilities and consequently poor sweep efficiency. Hence, polymer is usually added to increase water viscosity and reduce the mobility ratio between the aqueous and oleic phases in the reservoir (Hirasaki and Pope, 1974; Sorbie, 1991; Mishra et al., 2014; Samanta et al., 2012). The magnitude of the viscosity increase depends on the amount of the added polymer (or its concentration in the solution), which has a major impact on the economics of chemical enhanced oil recovery (EOR) projects. Moreover, an increase in the injectant viscosity reduces the well injectivity (maximum injectable flowrate for a given pressure drop), which can increase the life of the project (Glasbergen et al., 2015). Mechanical entrapment of the polymer molecules also increases with increasing polymer concentration (Farajzadeh et al., 2016; Lotfollahi et al., 2016). Therefore, the viscosity of the polymer solution should be designed such that the targeted oil is produced in a short time at a small cost. Although the addition of even small amounts of polymer will lead to an increase in oil recovery, compared to water or polymer solution with low viscosity, for *maximum utilization* of the injected polymer the displacement front should remain stable. To stabilize the displacement front minimum amount of polymer concentration (or polymer viscosity) is required.

The objective of this paper is to discuss this topic and review the available methods for designing the mobility control in chemical EOR processes. We focus on the design based on the shock mobility ratio and the method proposed by Gogarty et al. (1970). In the latter, the total mobility at the shock saturation is matched to the minimum total mobility in the reservoir (see Fig. 4). In both approaches the total mobility should be known at the front, which can be determined using fractional-flow theory, explained next. We neglect the effect of relative permeability hysteresis in this study.

2. Determination of the shock water saturation using fractional-flow theory

Fractional-flow theory is a useful one-dimensional tool in understanding the underlying physics of many EOR processes including polymer and surfactant flooding (Pope, 1980; Bedrikovetsky, 1993; Lake et al., 2014). In the absence of capillary and buoyancy forces, the fractional-flow function is

$$f_w = \frac{1}{1+\frac{\lambda_o}{\lambda_w}} = \frac{1}{1+\left(\frac{k_{rw}}{k_{ro}}\right)\left(\frac{\mu_o}{\mu_w}\right)} \tag{3}$$

where, $\lambda_\alpha = k_{r\alpha}/\mu_\alpha$ is the relative mobility of phase α. The displacing and displaced phases are denoted by *w* and *o*, respectively. A Corey-type function (Lake et al., 2014; Dake, 1978) is used to calculate the phase relative permeabilities:

$$k_{rw} = k_{rw}^e S_{wN}^{n_w} \text{ and } k_{ro} = k_{ro}^e\left(1-S_{wN}\right)^{n_o}$$
$$\text{with } S_{wN} = \frac{S_w - S_{wc}}{1-S_{orw}-S_{wc}} \tag{4}$$

The effect of the injected EOR agent is represented by an additional fractional-flow function constructed by modifying the input parameters to the original water–oil f_w function. For polymer flooding this change is usually represented by increasing the viscosity of the displacing aqueous phase, while for surfactant flooding (SP and ASP) the relative permeability curves change because of the reduction in the interfacial tension. Fig. 4 shows an example of the f_w vs. water saturation, S_w, and an ensuing water saturation profile for a polymer EOR process. The graphical solution of this problem consists of four steps: (1) identify injection point (*J*) and initial condition at the start of the EOR process (*I*) on the f_w curves, (2) draw the tangent line originating from point $(-D_s,0)$ to the polymer/oil f_w curve to obtain point *A*. The slope of this line gives the specific velocity of the chemical front, v_{cF}, (3) determine the intersection between the tangent line and water/oil f_w to obtain point *B*, and (4) connect point *B* to point *I* (the velocity of the oil-bank front, v_{oB}, is the slope of line *BI*). The retardation factor or the frontal delay caused by adsorption of the injected chemical can be calculated from the measured data:

$$D_s = \frac{1-\phi}{\phi}\frac{\rho_S}{\rho_w}\frac{\Gamma_S}{c_{inj}} \tag{5}$$

where, ϕ is the porosity, ρ_S is the rock (grain) density, ρ_w is the density of the polymer (or surfactant) solution, Γ_S is the adsorbed chemical on rock measured in the unit of $\left(\frac{\mu g}{gr\ rock}\right)$ and c_{inj} is the injected concentration of chemical expressed in ppm. The inclusion of adsorption in the calculations changes the positions of points *A* and *B* on the fractional-flow curves such that the velocity of the chemical front decreases resulting in delayed propagation of the chemical front.

As can be seen from Fig. 4 there are two fronts during the chemical EOR process: the oil-bank front, behind which initial water in the system (including the chemical slug denuded of chemicals because of adsorption) displaces oil, and the chemical front behind which the injected chemical pushes the oil towards the outlet. The stability of the oil-bank front depends on the initial conditions of the reservoir (especially the initial oil or water saturation, which is frequently not constant in a real reservoir) as well as the (drainage) relative permeability parameters. However,

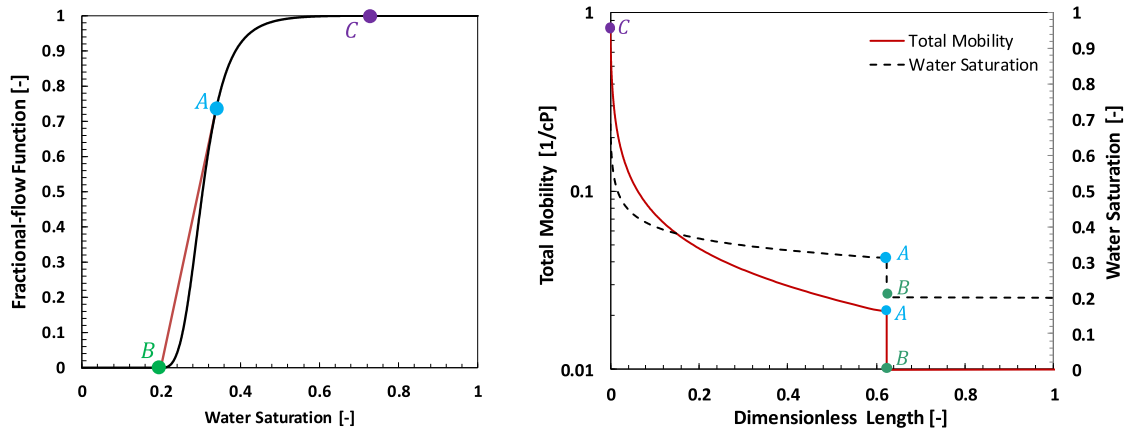

Fig. 1. An example of water fractional-flow function as a function of the water saturation and the constructed 1-D Buckley–Leverett saturation profile at $t_D = 0.12$ PV. The total relative permeability profile is obtained from Eq. (1).

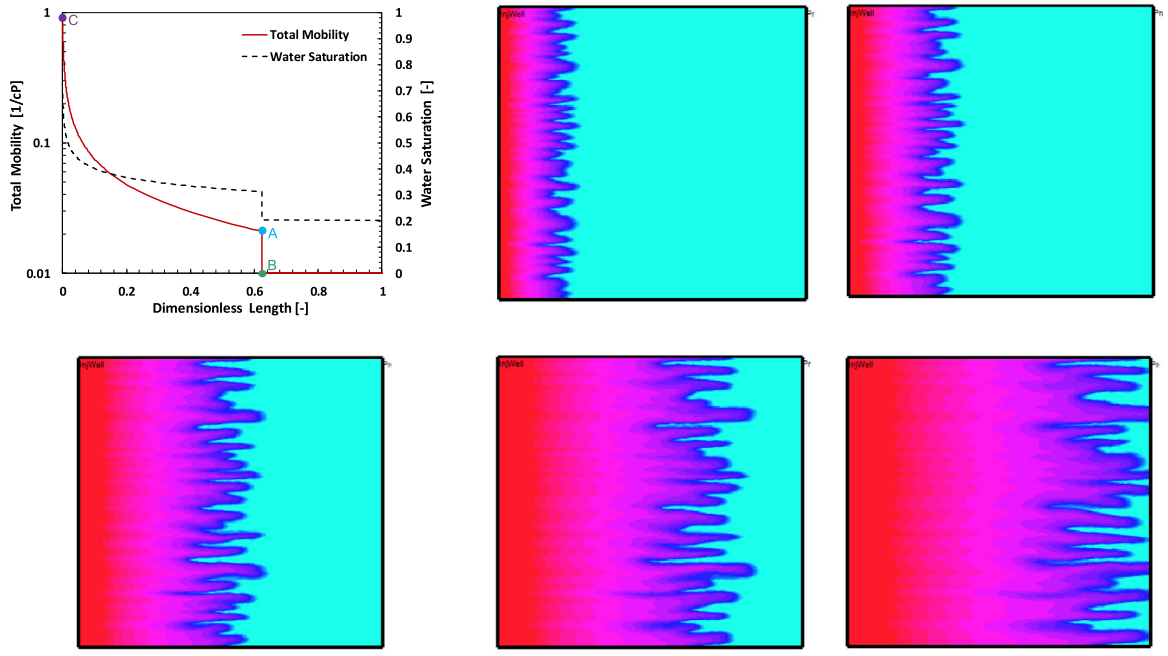

Fig. 2. Displacement of oil by water for a case with shock mobility ratio of 2.

this is inherent in the process and cannot be easily modified externally. Therefore, the design of mobility control only concerns the stability of the chemical front. The stability of this front is governed by the viscosity ratio between the injected chemical and the oil, the (original and modified) relative permeability parameters, and adsorption. In fact, any parameter in the fractional-flow function that changes positions of points A and B in Fig. 4 has an impact on the stability of the chemical front. The initial water saturation (point I in Fig. 4) is not relevant for the stability of this front.

In summary, to ensure a stable displacement, the mobility of the chemical (polymer or surfactant polymer) slug should be smaller than that of the oil bank that precedes it. To satisfy this condition, the total mobility at the shock water saturation (λ_T^A) should not be greater than the total mobility at intersection point B (λ_T^B). This is method 1 in the paper. The design suggested by Gogarty et al. (method 2) is more conservative and requires λ_T^A be less than that of the minimum total mobility across the saturation range ($\lambda_{T,min}$).

It is usually assumed that the presence of polymer does not alter the original water/oil relative permeability function; therefore, for the polymer flooding the main design parameter is the small-shear rate viscosity of the injected solution. However, for surfactant flooding, where the reduction in the interfacial tension (IFT) between the oil and water leads to an increase in the relative permeability or mobility of both phases, the viscosity and interfacial tension can be simultaneously modified to warrant a stable front. The design based on method 1 is the minimum requirement of the front stability.

Finding the polymer viscosity to satisfy the stability condition in Eq. (2) is an iterative process because the position of both points A and B depend on the polymer/oil fractional-flow curve which in turn requires the polymer viscosity as an input parameter. For method 2, since the saturation at point B is fixed, one only needs to obtain the saturation at point A from the fractional-flow curve, which is also an iterative process. For both methods the convergence is quite fast, if the initial guess is close to the final value. The *Solver* functionality in Microsoft-Excel can be used. Next, we provide some examples and discuss the ensuing results.

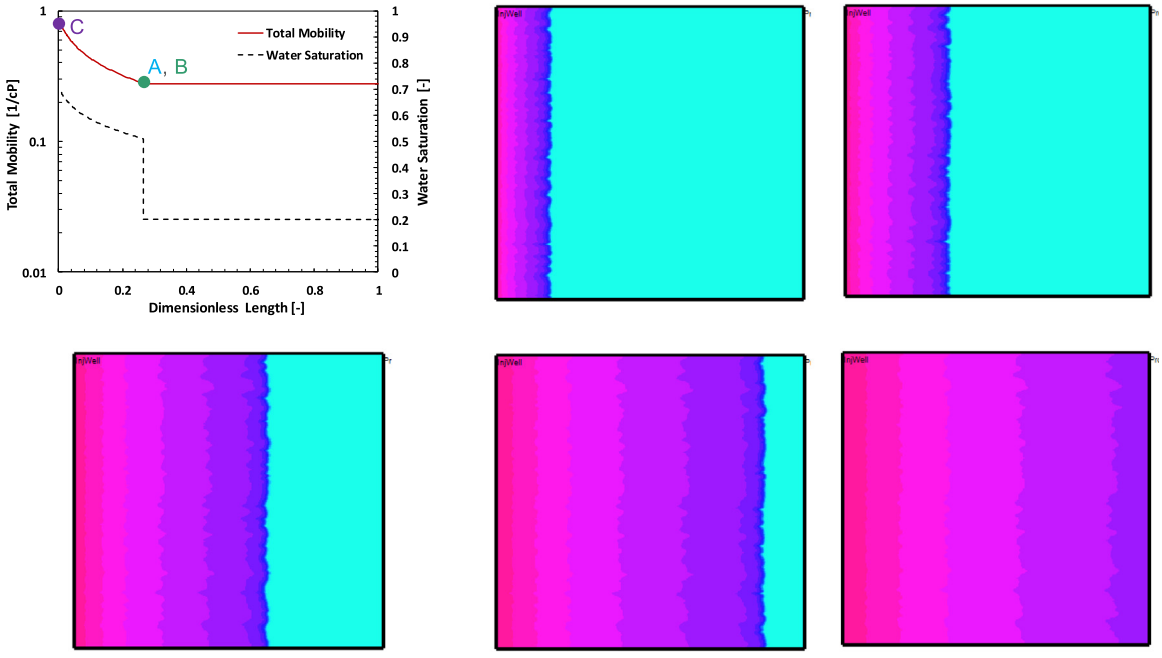

Fig. 3. Displacement of oil by water for a case with shock mobility ratio of 1.

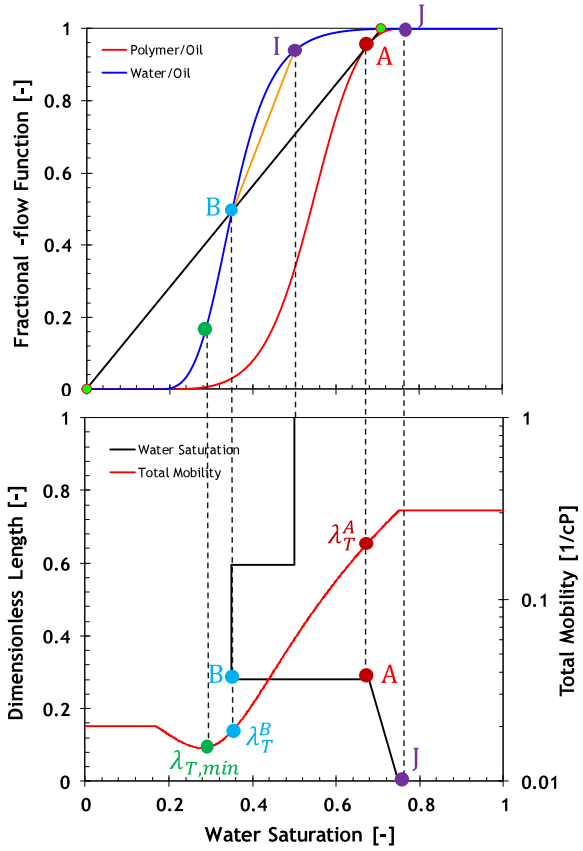

Fig. 4. The fractional-flow function vs. water saturation (top) and the constructed water-saturation profile and total mobility as function of water saturation (bottom). The adsorption is assumed to be zero here.

3. Case I: Polymer flooding, no adsorption

We consider the design of polymer-flooding an oil with viscosity of 90 cP. It is assumed that the water-oil relative permeability remains unchanged during the oil displacement by polymer. The relative permeability parameters are in Table 1. Following the iterative procedure explained in the previous section the minimum polymer viscosity required to guarantee a stable displacement front is calculated to be 8.0 cP (method 1). The design based on method 2 gives polymer viscosity of 12.0 cP. Using these values, the corresponding fractional-flow curves, and water saturation and total mobility profiles (after 0.25 pore volume of polymer injection) are plotted in Fig. 5. The total mobility upstream of the chemical front (point *A*) is larger than that of the downstream (point *B*) for method 2, which results in a shock mobility of 0.84. For method 1 these points lie on top of each other by design. Moreover, the different polymer viscosities result in different saturation profiles: the shock water saturation rises from 0.52 in method 1 to 0.55 in method 2, which implies a larger displacement efficiency for method 2. The increase in the polymer viscosity, shifts point *A* closer to point *1-*S_{orc}, which is desirable in terms of oil recovery. However, one should evaluate the cost and consequences of injection of larger polymer concentrations and compare it to the additional oil obtained. For shock water saturation to equal 1-S_{orc}, extremely high viscosities are required, for example, for the parameter considered here one should increase the polymer viscosity to more than 5000 cP, which is far from practical.

4. Case II: Polymer flooding, effect of adsorption

When adsorption is considered, the tangent line to the polymer/oil f_w curve originates from $(-D_s,0)$, see Eq. (5). D_s, the retardation factor (or frontal advance loss) defined by Eq. (5), is the additional pore volume of the polymer solution needs be injected to satisfy the rock adsorption. It results in different chemical front and oil-bank saturations (and velocities). Basically, adsorption delays propagation of the chemical front (and to a lesser degree the oil-bank front). The change in the positions of

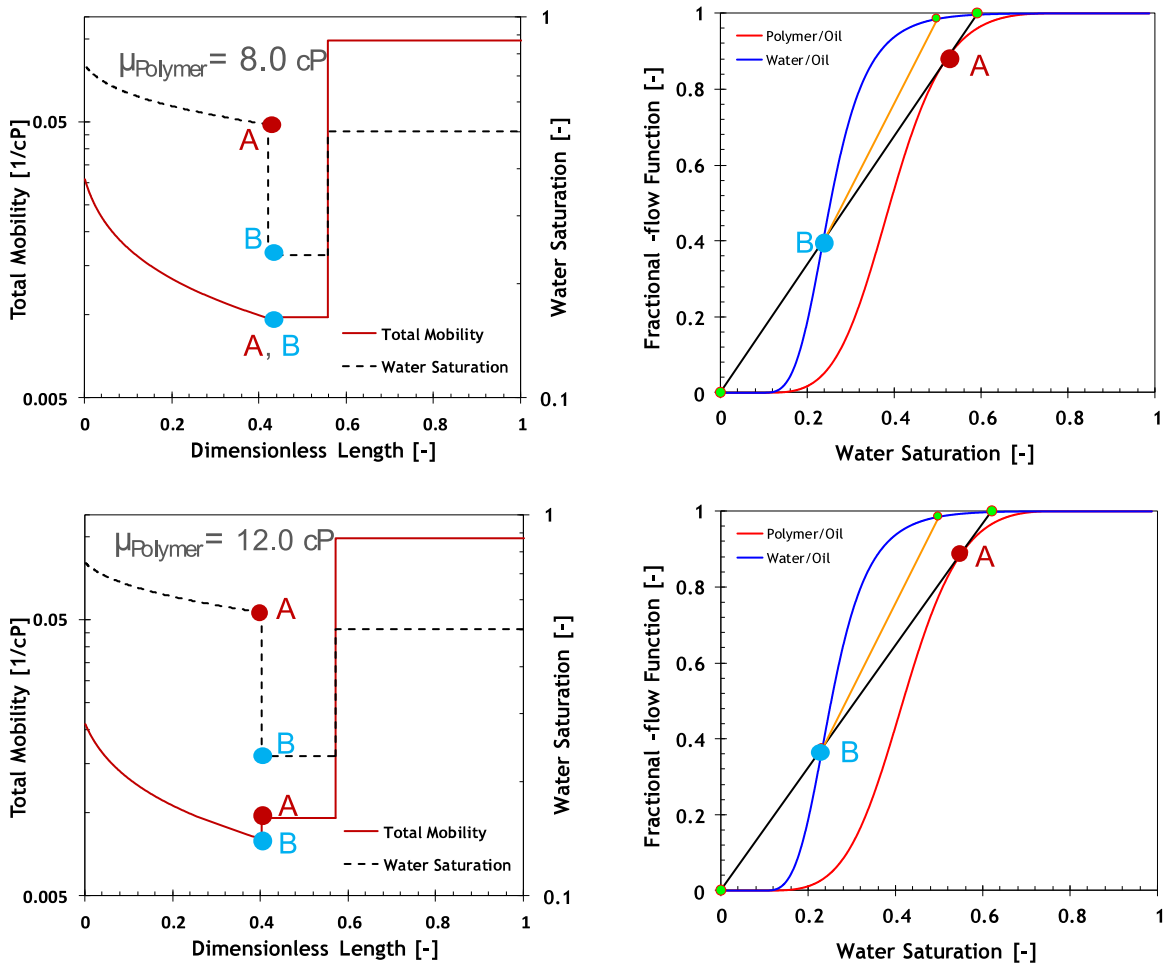

Fig. 5. The fractional-flow curves, and water saturation and total mobility profiles: matching the shock mobility ratio (top) and using Gogarty et al. method (bottom). The input parameters are in Table 1. The profiles are plotted for dimensionless time of 0.25 PV.

Table 1
Relative permeability parameters and viscosity of the fluids.

n_w	3
n_o	2
${k_{rw}}^e$	0.25
${k_{ro}}^e$	0.85
S_{ori}	0.5
S_{orw}	0.25
S_{wc}	0.10
μ_w	0.65 cP
μ_o	90 cP

points *A* and *B* results in different fluid mobilities at the shock front and the oil bank. Fig. 6 illustrates the effect of adsorption ($D_s = 0.3$) on the saturation and the mobility profiles. The same parameters as in Table 1 are used here. Using method 1, the minimum viscosity for the front stability is calculated to be 6 cP, which is smaller than the no-adsorption case. This is because the shock and the oil-bank water saturations increase from 0.52 and 0.23 to 0.54 and 0.28, respectively. The change in both saturations leads to greater total fluid mobility at the polymer front and the oil bank for adsorption case. Moreover, when polymer adsorbs on rock, a larger volume of water displaces the oil. Using method 2 results in a different scenario. With inclusion of adsorption, when the polymer front is matched to the minimum total mobility, more polymer should be used in the flood. In the case considered, the polymer viscosity should be increased from 12 cP to 16 cP. Accordingly, the water saturations at the chemical and oil-bank

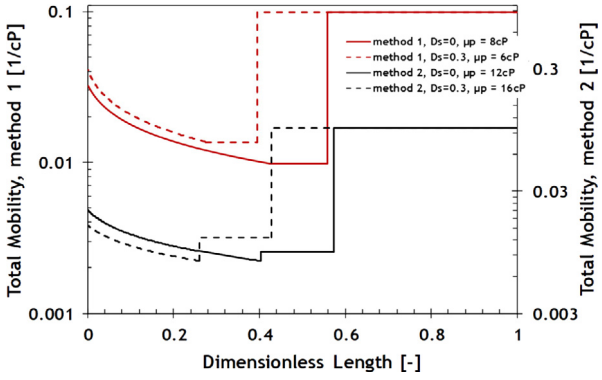

Fig. 6. The profiles of total fluid mobility for the cases with and without adsorption ($D_s = 0.3$). All the profiles are plotted after 0.25 PV of polymer injection.

fronts increase from 0.55 and 0.23 to 0.61and 0.27, respectively. Note that in method 2, the denominator in Eq. (2) is fixed and adsorption only affects the mobility in the nominator. Also, in this scenario, behind the chemical front the total fluid mobility for the case of adsorption is less than that of the no-adsorption case (see Fig. 6). However, the oil bank has higher mobility in the adsorption case, similar to method 1.

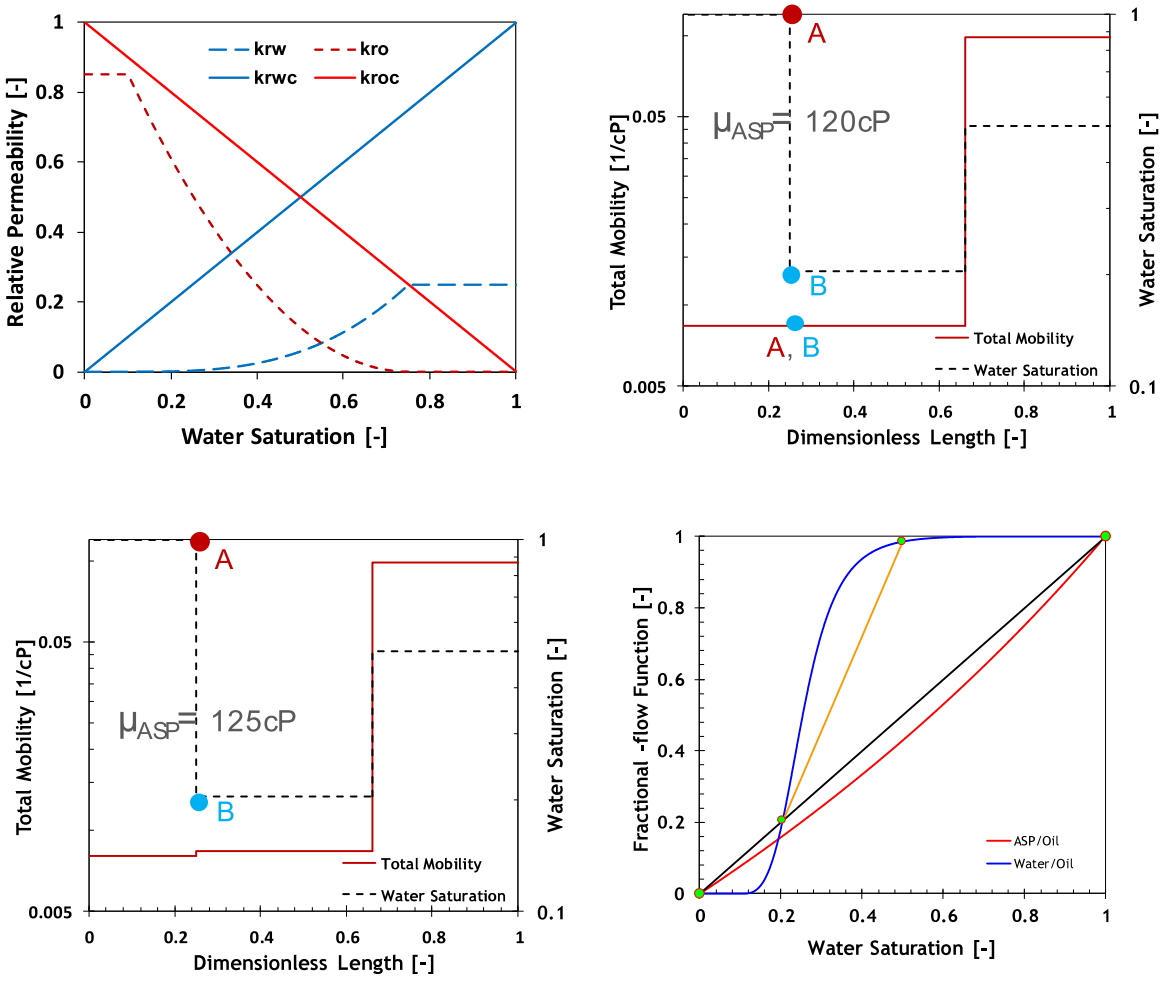

Fig. 7. The original and scaled relative-permeability curves for an ASP displacement with ultra-low IFT of less than 0.005 mN/m (a); water saturation and total mobility profiles for $\mu_{ASP} = 120$ cP (b) and $\mu_{ASP} = 125$ cP (c) obtained using method 1 and method 2, respectively. The fractional flow function vs. saturation using $\mu_{ASP} = 120$ cP (d).

5. Case III: Surfactant flooding

The modelling of surfactant flooding using fractional-flow theory requires simplifying assumptions. Firstly, the formation of Winsor type III microemulsion phase is ignored to allow the description of the process by only two phases. The microemulsion phase generally has a larger viscosity than the oil. Secondly, the properties of the surfactant-polymer (SP) or the alkali-surfactant-polymer (ASP) slug are assigned to the displacing aqueous phase. In the simplest form, the solubilization of oil in water and swelling of oil by water droplets are also neglected, although the inclusion of these mechanisms is possible (Larson and Hirasaki, 1978). Finally, the only mechanism of oil recovery is the increase of the capillary number (the ratio between the viscous and capillary forces), mainly by reduction of the interfacial tension between oil and water (γ_{ow}). Consequently, the original water/oil relative permeability parameters depend on capillary number or γ_{ow}. Here, we use the scaling method proposed by Liu et al. (2010) to construct the ASP/oil fractional-flow curves. It is assumed that when $\gamma_{ow} > 1$ mN/m surfactant will have no effect on the oil recovery and hence the original water/oil relative permeability parameters are used. When $\gamma_{ow} < \gamma_{ow}^{crit} = 0.005$ mN/m, the capillary number becomes very large and surfactant has a 100% displacement efficiency. Therefore,

$$n_{wc} = n_{oc} = 1,\ S_{orc} = S_{wcc} = 0,\ k^e_{rwc} = k^e_{roc} = 1 \quad \text{for } \gamma_{ow} < \gamma_{ow}^{crit} = 0.005 \text{ mN/m} \tag{6}$$

For $\gamma_{ow}^{crit} \le \gamma_{ow} \le 1$ the following relations hold:

$$n_{wc} = n_w + \frac{1}{6}\log 10\ \gamma_{ow},\ n_{oc} = n_o + \frac{1}{6}\log 10\ \gamma_{ow}$$

$$S_{orc} = S_{orw}\left(1 + \frac{\log 10\ \gamma_{ow}}{2.3}\right),\ S_{wcc} = S_{wc}\left(1 + \frac{\log 10\ \gamma_{ow}}{2.3}\right) \tag{7}$$

$$k^0_{rwc} = k^0_{rw} + \left(1 - k^0_{rw}\right)\frac{(S_{orw} - S_{orc})}{S_{orw}},$$

$$k^0_{roc} = k^0_{ro} + \left(1 - k^0_{ro}\right)\frac{(S_{wc} - S_{wcc})}{S_{wc}}$$

Using these relations, we explore the requirements of the mobility control in the SP or ASP projects in this section. In the first case we assume that the ASP solution is injected at optimum conditions, i.e., the interfacial tension is well below $\gamma_{ow}^{crit} = 0.005$ mN/m. The relative-permeability curves then become two straight lines, as illustrated in Fig. 7a. Again, the parameters listed in Table 1 are used in the calculations. When the phase relative permeabilities are straight lines, the end-point mobility ratio becomes 1. Then, it is generally assumed that matching the ASP and oil viscosity guarantees a stable displacement. However, using both methods for this case ensues ASP viscosities that are larger than the oil viscosity. This is because of the smaller mobility of the oil bank (point B) compared to the mobility of the chemical front (point A). Also, in this case the mobility at point B is close to the

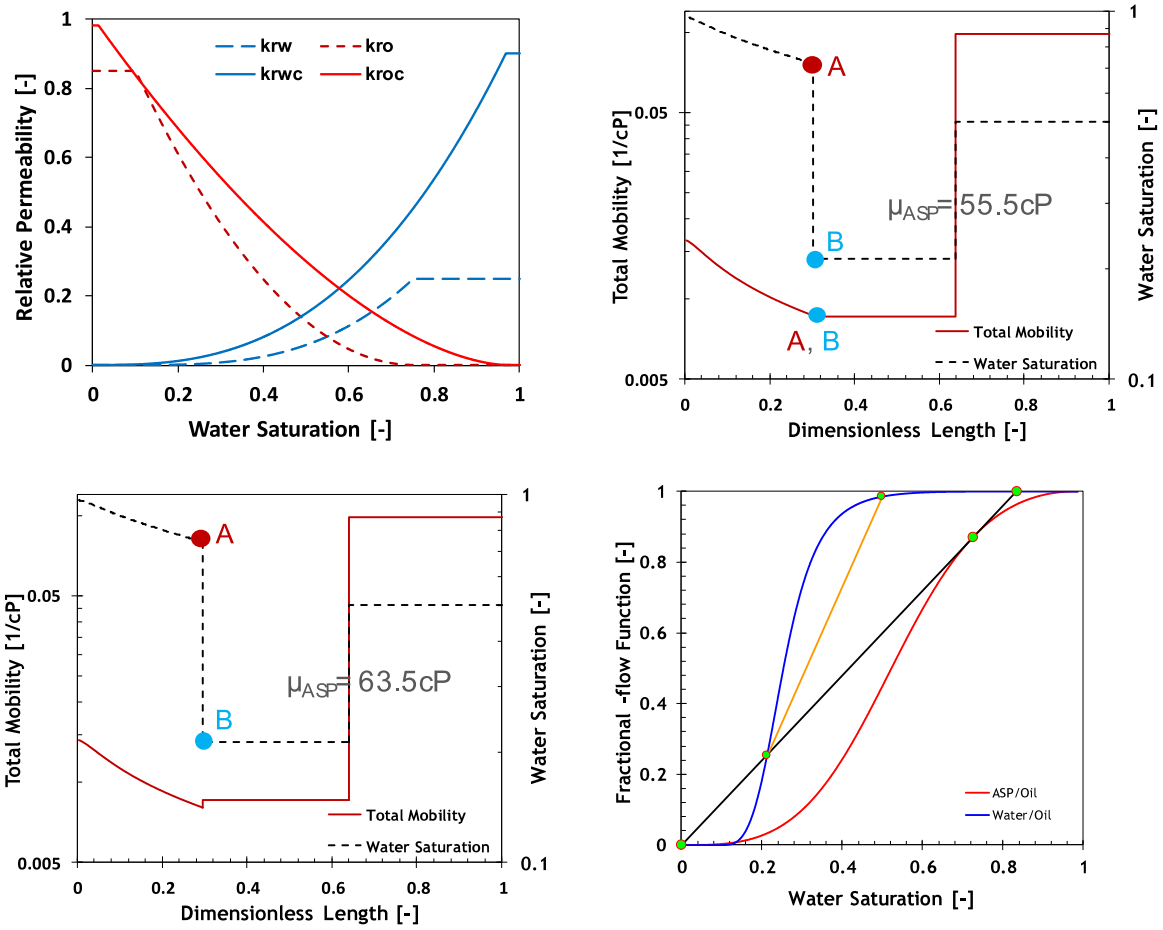

Fig. 8. The original and scaled relative permeability curves an ASP displacement IFT of 0.01 mN/m (a); water saturation and total mobility profiles (at $t_D = 0.25$ PV) for $\mu_{ASP} = 55.5$ cP (b) and $\mu_{ASP} = 63.5$ cP (c) obtained using method 1 and method 2, respectively. The fractional flow function vs. saturation using $\mu_{ASP} = 55.5$ cP (d).

minimum total mobility across the saturation range. Therefore, the results obtained from the two methods are not significantly different (120 vs. 125 cP).

The second case considers injection of a Winsor type I ASP solution with $\gamma_{ow} = 0.01$ mN/m. Since the interfacial tension is not ultra-low, the scaled relative permeability curves are not straight lines, as shown in Fig. 8a. The curvature in the relative permeability function is an indication that the capillary forces are still significant (although smaller than the original capillary number). It is notable that, when γ_{ow} is not ultra-low, less polymer is required to obtain a stable displacement front. This is because of the stabilizing effect of capillary forces, manifested in non-straight relative permeability curves. Similar to the polymer injection, when method 2 is used the ASP solution should be injected with higher viscosity (~64cP). Once again, the economic trade-off between more oil (in the case of ultra-low IFT) and large amounts of polymer required to stably displace the oil bank should be considered.

Fig. 9 illustrates the effect of oil viscosity on the design of mobility control in the ASP process. The water/oil relative permeability parameters in Table 1 are scaled using Eqs. (6) and (7) depending on the value of γ_{ow}. It appears that for Winsor type III injection (ultra-low IFT), the polymer viscosity is the ASP slug should be always larger than the oil viscosity. For the under-optimum or Winsor type I ASP solution, for oils with medium and large viscosity the required polymer viscosity is smaller than that of the oil due to beneficial effects of the relative permeability on the front stability. The difference between method 1 and method 2 is marginal for oils with low viscosity (light oils). Remarkably, for light oils the required polymer viscosity is significantly larger than the oil viscosity. For example, for the oil with viscosity of 2 cP, the viscosity of the ASP solution should not be less than 5 cP for $\gamma_{ow} = 0.01$ mN/m or 7 cP for $\gamma_{ow} = 0.001$ mN/m. This has major (economic) consequences for the application of the ASP process for the light oils.

6. Polymer utilization

The 1-D calculations of the fractional-flow theory provide an estimate of the displacement efficiency of the processes. Upscaling of the results to field scale requires knowledge on the extent of the spatial heterogeneity of the reservoir. To investigate the implications of the outcome of this study, the modified Koval approach is used to obtain an approximate oil-production history for polymer and ASP injection. The modified Koval method assumes that both the chemical and oil-bank fronts are spread out because of the heterogeneity of the porous medium or the adverse mobility ratio and gravity effects (Mollaei and Delshad, 2011; Jain and Lake, 2013). The extent of non-ideality or deviation from the results of the 1-D analytical method is quantified by two Koval factors, K_{oB} for the oil bank and K_c for the chemical front, which are functions of the Dykstra–Parsons coefficient and (possibly) the mobility ratio between the displacing and displaced fluids (Lake et al., 2014; Farajzadeh et al., 2012). The main consequences of the non-ideal displacement are (much) earlier breakthrough of the oil and chemical fronts, smaller oil cuts, and elongated production times (red curves in Fig. 10).

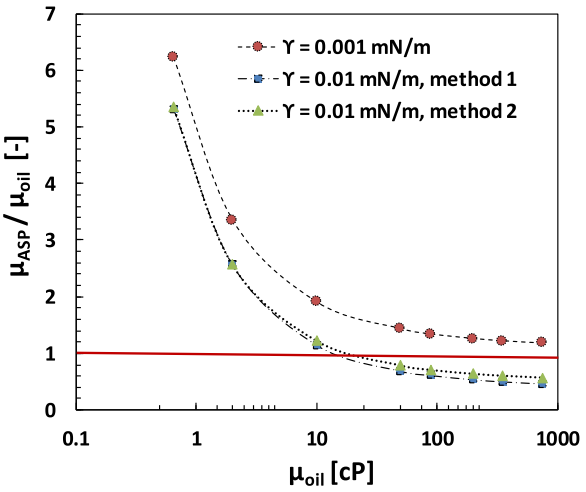

Fig. 9. Effect of oil viscosity on the design of viscosity of an ASP solution. The original water/oil relative permeabilities summarized in Table 1 and the scaling relations in Eqs. (6) and (7) are used in the calculations.

Fig. 11a depicts the history of the upscaled oil recovery factor for the polymer flooding with viscosity of 8 cP two ASP floods with $\gamma_{ow} = 0.01$ mN/m and $\gamma_{ow} = 0.001$ mN/m. In all three cases a Koval factor of 5 is used for the oil-bank front. For the polymer flood, the Koval factor for the chemical front, (K_c) is assumed to remain the same since the viscosity is small. For the ASP floods, $K_{cF} = 4$ and $K_{cF} = 3$ is assigned for polymer viscosity of 56cP and 120 cP, respectively to account for the positive impacts of the higher injection viscosities on the performance of the flood. The oil recovery for ASP with ultra-low IFT is the highest because of its better displacement efficiency and for the polymer injection is the lowest. To compare the results, a Polymer Utilization Factor (PUF) is plotted for the three cases, Fig. 11b. The PUF is defined as the volume of the produced oil per mass of the injected polymer (bbl/kg polymer) it is be used as proxy for more lengthy economic calculations. From available data, to prepare polymer solutions with viscosities of 8, 56, and 120 cP, polymer concentrations of 600, 1300, and 2500 ppm should be used. In the ASP calculations, other chemicals are ignored (even though surfactant unit costs usually surpasses that of polymer). The calculated PUFs in Fig. 11b agree well with the PUFs reported for field application of polymer flooding, which on average are 2–3 bbl/kg polymer (Sheng et al., 2015). Fig. 11 indicates that the PUF is the largest for the polymer injection even though the oil recovery is the lowest. In contrary, for the ASP flood with ultra-low IFT, despite the large oil recovery, the PUF is the lowest. The main difference between polymer and ASP is the recovery of the capillary trapped oil, which can add oil volumes to the reserves.

7. Conclusions

This study compares two methods of mobility-control design for chemical enhanced oil recovery processes. Method 1 matches the total relative fluid mobility upstream and downstream of the shock front. In method 2 the viscosity of the displacing agent is selected such that the total mobility at the shock water saturation is equal to or less than the minimum mobility across the saturation range. The two methods are based on fractional flow analysis of one-dimensional flow and they are validated against two-dimensional simulations of flow through heterogeneous permeable media.

The following conclusions are made:

- Accurate measurement of the water/oil relative permeability curves is key for the design of mobility control in polymer and surfactant/polymer flooding.
- The polymer viscosity obtained by setting the shock-front mobility ratio to one (method 1) is the minimum viscosity to ensure a stable displacement front. Injection of a polymer solution with a viscosity less than this will result in fingering and bypassing of oil.
- Design by method 2 results in a larger viscosity than method 1. This shifts the shock water saturation to larger values and hence more oil is displaced.
- When polymer adsorption is considered, a small polymer viscosity is required to stabilize the front based on method 1. This is the result of the lost polymer in the region ahead of the delayed polymer front, which increases the total mobility of the oil bank (because of changes in saturations). Therefore, less polymer is required to displace the oil bank.
- Inclusion of adsorption does not affect the minimum mobility across the saturation range but increases the shock mobility. Consequently, a larger polymer viscosity is required to satisfy the conditions of method 2.
- The straightening of relative-permeability functions during alkali-surfactant-polymer (ASP) or surfactant-polymer (SP) flooding leads to increased polymer viscosity in the main and chase slugs.
- Injection of Winsor Type I, or under-optimum surfactant solutions, which cause moderate reductions in the interfacial tension, reduces the polymer viscosity required for stable displacement.

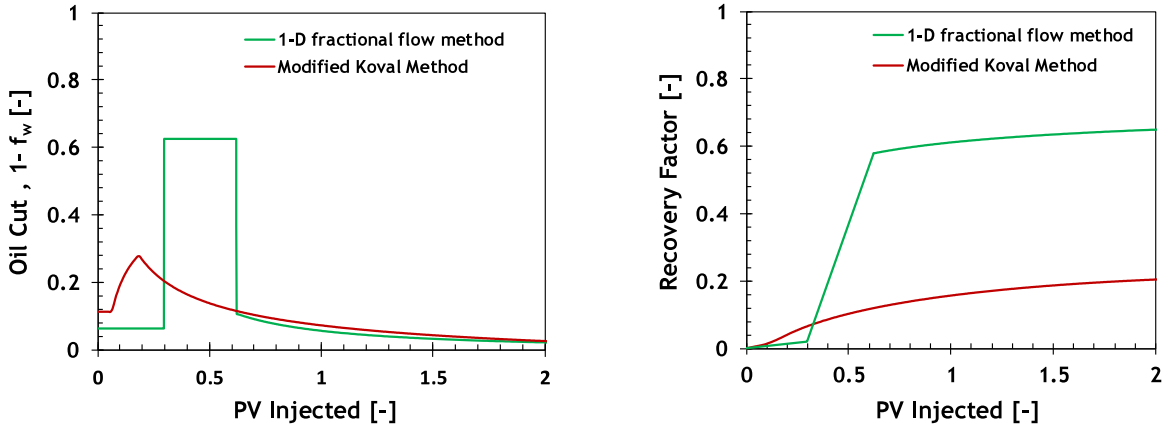

Fig. 10. The 1-D oil cut and oil recovery histories obtained from fractional-flow theory compared to the upscaled histories using modified Koval approach with $K_{oB} = K_{cF} = 5$. (For interpretation of the references to colour in this figure legend, the reader is referred to the web version of this article.)

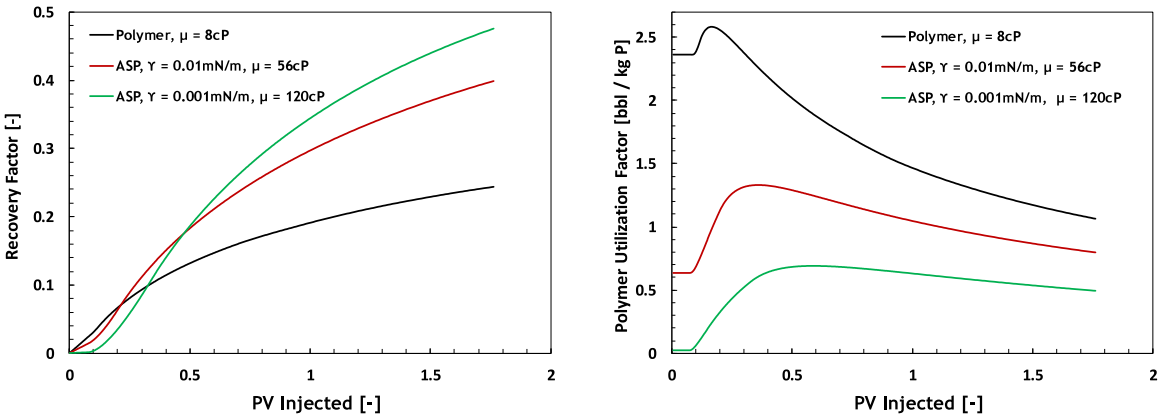

Fig. 11. Upscaled oil recovery histories for the three cases considered (left) and the calculated polymer utilization factor history (right).

- For ASP solutions with ultra-low interfacial tension (IFT) reduction (Winsor type III), the required polymer viscosity is always greater than the oil viscosity (at low shear rates). However, for Winsor type II solution, for oils with medium and large viscosity the non-linear shape of the relative permeability function leads to polymer viscosities that are less than that of the oil.
- For light oils the viscosity of the ASP solution should be significantly larger than the oil viscosity.
- Despite lower ultimate oil recovery, for the same slug size of polymer and ASP slugs, the polymer utilization factor (i.e. the volume of oil produced per unit mass of polymer injected) is greater for polymer flooding compared to the ASP flooding.

References

Bedrikovetsky, P., 1993. Mathematical Theory of Oil & Gas Recovery, with Applications To Ex-USSR Oil & Gas Condensate Fields. Kluwer Acad. London.

Chouke, R.L., Stability analysis for a secondary miscible displacement with an initially sharp solvent-oil interface. In: Proceedings of the Society of Petroleum Engineers/Department of Energy Third Joint Symposium on Enhanced Oil Recovery, Tulsa, Oklahoma (Society of Petroleum Engineers, Dallas, Texas, 1982), SPE-10686, Appendix B of J. W. Gardner and J. G. J. Ypma.

Dake, L.P., 1978. Fundamentals of Reservoir Engineering. Elsevier, N. Y.

Farajzadeh, R., Eftekhari, A.A., Hajibeygi, H., Kahrobaei, S., van der Meer, J.M., Vincent-Bonnieu, S., Rossen, W.R., 2016. Simulation of instabilities and fingering in surfactant alternating gas (SAG) foam enhanced oil recovery. Journal of Natural Gas Science and Engineering 34 (2016), 1191–1204.

Farajzadeh, R., Ranganathan, P., Zitha, P.L.J., Bruining, J., 2012. The effect of heterogeneity on the character of density-driven natural convection of co2 overlying a brine layer. Adv. Water Resour. 34 (3).

Glasbergen, G., Wever, D., Keijzer, E., Farajzadeh, R., 2015. Injectivity loss in polymer floods: causes, preventions and mitigations. In: SPE 175383. SPE Kuwait Oil and Gas Show and Conference.

Gogarty, W.B., Meabon, H.P., Milton, H.W., 1970. Mobility control design for miscible-type waterfloods using micellar solutions. J. Pet. Technol. 22 (02).

Hirasaki, G.J., Pope, G.A., 1974. Analysis of factors influencing mobility and adsorption in the flow of polymer solutions through porous media. Soc. Pet. Eng. J. 14, 337–346.

Homsy, G.M., 1987. Viscous fingering in porous media. Ann. Rev. Fluid Mech. 19, 271–311.

Jain, L., Lake, L.W., 2013. Upscaling of miscible floods: an extension to Koval's theory. In: SPE-166400-MS, SPE Annual Technical Conference and Exhibition, 30 September-2 October. New Orleans, Louisiana, USA.

Lake, L.W., Johns, R.T., Rossen, W.R., Pope, G.A., 2014. Fundamentals of Enhanced Oil Recovery. Soc. of Pet. Eng, Richardson, Tex.

Larson, R.G., Hirasaki, G.J., 1978. Analysis of the physical mechanisms in surfactant flooding. SPE J. 18 (01), 41–58.

Liu, S., Li, R.F., Miller, C.A., Hirasaki, G.J., 2010. Alkaline surfactant polymer processes: Wide range of conditions for good recovery. SPE J. (2010), 282–293.

Lotfollahi, M., Farajzadeh, R., Delshad, M., Al-Abri, A.K., Wassing, B.M., Al-Mjeni, R., Awan, K., Bedrikovetsky, P., 2016. Mechanistic simulation of polymer injectivity in field tests. SPE J. 21 (04), 1, 178-1, 191.

Mishra, S., Bera, A., Mandal, A., Effect of Polymer Adsorption on Permeability Reduction in Enhanced Oil Recovery. J. Pet. Eng., Volume 2014, Article ID 395857.

Mollaei, A., Delshad, M., 2011. General isothermal enhanced oil recovery and waterflood forecasting model. In: SPE 143925, Presented At SPE Annual Technical Conference and Exhibition, 30 Oct.-2 Nov. Denver, Colorado, USA.

Pope, G.A., 1980. The application of fractional flow theory to enhanced oil recovery. SPE J. 20 (03), 1980.

Riaz, A., Tchelepi, H.A., 2004. Linear stability analysis of immiscible two-phase flow in porous media with capillary dispersion and density variation. Phys. Fluid (16), 4727.

Riaz, A., Tchelepi, H.A., 2006. Influence of relative permeability on the stability characteristics of immiscible flow in porous media. Transp. Porous Media 64, 315–338.

Samanta, A., Bera, A., Ojha, K., Mandal, A., 2012. Comparative studies on enhanced oil recovery by alkali–surfactant and polymer flooding. J. Pet. Explor. Prod. Technol. 2 (2), 67–74, | Cite as.

Sheng, J.J., Bernd, L., Azri, N., 2015. Status of polymer flooding technology. SPE J. 54 (02).

Sorbie, K.S., 1991. Polymer-Improved Oil Recovery. CRC Press, Boca Raton, Fla.